Membrane Transport in Hepatic Clearance of Drugs II: Zonal Distribution Patterns of Concentration-Dependent Transport and Elimination Processes

Younggil Kwon[1,2] and Marilyn E. Morris[1,3]

Received December 3, 1996; accepted March 20, 1997

Purpose. The objective of the present simulation study was to investigate the effects of hepatic zonal heterogeneity of membrane transporter proteins and intrinsic elimination activities on hepatic clearance (*CL*) and drug concentration gradient profiles in the sinusoidal blood and hepatocytes.

Methods. The model used in the simulations assumes an apparent unidirectional carrier-mediated transport and a bidirectional diffusion of substrates in the hepatic sinusoidal membrane as well as a nonlinear intrinsic elimination. Three different distribution patterns of the transporter and the metabolizing enzyme along the sinusoidal flow path were used for the simulations. The effects of changes in the Michaelis-Menten parameters for those nonlinear processes, and in the unbound fractions of the drug in blood and tissue components were investigated.

Results. Significant differences in *CL* occurred when the distribution patterns of the transporter and/or the metabolizing enzyme activities were altered under nonlinear conditions. The highest *CL* values were observed when the transporter and the metabolizing enzyme had similar distribution patterns within the liver acinus, while opposite distribution patterns produced the lowest *CL* values. Tissue concentration profiles were significantly affected by the distribution patterns of the transporter, but the changes in blood concentration profiles were relatively small. Altering protein binding in blood produced significant changes in *CL*, and blood and tissue concentration gradients, while altering protein binding in tissue affected only drug accumulation patterns within hepatocytes, regardless of the distribution patterns of the transporter or the metabolizing enzyme.

Conclusions. The present simulations demonstrate that hepatic zonal heterogeneities in the transporter and the metabolizing enzyme activities can significantly influence hepatic clearance and/or drug concentration gradient profiles in the sinusoidal blood and hepatocytes.

[1] Department of Pharmaceutics, School of Pharmacy, State University of New York at Buffalo, Amherst, New York 14260.

[2] Drug Metabolism Department, Central Research Division, Pfizer Inc., Groton, Connecticut 06340.

[3] To whom correspondence should be addressed. (e-mail: memorris@ acsu.buffalo.edu)

GLOSSARY $C_{s,x}$, $C_{t,x}$, substrate concentration in sinusoidal blood and hepatocytes at any given point x along the sinusoidal blood flow path of L ($0 \leq x \leq L$), respectively; *CL*, hepatic clearance; $CL_{1,x}$, $CL_{2,x}$, $CL_{3,x}$, $CL_{d,x}$, uptake, efflux, intrinsic and diffusional clearance at x, respectively; f_b, f_t, fraction of drug unbound to blood and tissue components, respectively; $K_{m,1}$, $K_{m,3}$, Michaelis-Menten constant of the transporter and metabolizing enzyme, respectively; L, length of the sinusoidal blood flow path; Q, blood flow rate; $V_{max,1}$, $V_{max,3}$, maximum capacity of the transporter and metabolizing enzyme, respectively; $V_{max,1,x}$, $V_{max,3,x}$, capacity of the transporter and metabolizing enzyme at x, respectively.

KEY WORDS: pharmacokinetic models; nonlinear transport; nonlinear intrinsic elimination; zonal distribution; blood and tissue concentration gradient profiles.

INTRODUCTION

Hepatic parenchymal cells are known to display various histochemical and functional heterogeneities in relation to their location in the liver acinus (1,2). Well documented are the zonal differences in metabolic functions of hepatocytes (1–4). Investigations have indicated that there are also intrinsic zonal heterogeneities in membrane transport abilities of hepatocytes for various endogenous and exogenous compounds, including bile acids (6), amino acids (7), dibromosulfophthalein (8,9), cysteine (10), ouabain (8) and rhodamine B (11). For instance, it has been demonstrated that the sodium-dependent uptake of taurocholic acid is more active in zone 1 (periportal region) than in zone 3 (perivenous region), while the sodium-independent transport is more active in zone 3 than in zone 1 (6). Studies on zonal differences in the uptake of several fluorescent compounds into acinar hepatocytes in the rat (12) have demonstrated distinct concentration gradient profiles of different substrates along the hepatocyte acinus varying from a consistent decline to a flat distribution or even a gradual increase from zone 1 to zone 3; these concentration profiles were dependent on the infusion concentrations. This reversed cellular gradient, which has also been reported in other studies (11,13), suggests that uptake processes are not homogeneously distributed along the hepatic acinus.

Computer simulation studies by Sato *et al.* (15) have demonstrated that in the presence of a diffusional barrier the extraction ratio of substrates was significantly affected by the distribution patterns of intrinsic metabolizing enzyme activity. The effect of various distribution patterns for metabolizing enzymes has also been examined in the absence of a transport barrier (16,17). However, the assumptions of these models regarding hepatic transport, i.e., a simple diffusional barrier or no barrier (instant equilibrium of drug between sinusoidal blood and hepatocytes) may not be physiologically relevant for many organic anions and cations, since *in vitro* and *in vivo* hepatic transport studies have demonstrated the presence of several distinct facilitated carrier-mediated transport systems for various endogenous and exogenous substrates (18,19). Additionally, although several pharmacokinetic studies have evaluated the influence of membrane transport and/or intrinsic elimination (metabolism and biliary excretion) for certain drugs under linear conditions (20,21), little is known concerning the influence of zonal differences in uptake and elimination processes on the apparent hepatic clearance or the concentration gradient profiles in blood and hepatocytes under nonlinear conditions.

The purposes of the present simulation study were to investigate 1) the effects of zonal heterogeneities of a carrier-mediated membrane transport system and a capacity-limited metabolizing process, 2) the effects of changes in Michaelis-Menten parameters for those nonlinear processes, and 3) the effects of blood and tissue protein binding, on clearance and concentration gradient profiles of substrates in sinusoidal blood and hepatocytes.

THEORY

The present simulation study uses an extended parallel tube model with capacity-limited sinusoidal uptake as well as

0724-8741/97/0600-0780$12.50/0

capacity-limited elimination (model II described in the accompanying paper, 22). In brief, the model is composed of two compartments: the sinusoid and hepatocyte. The liver is viewed as parallel sinusoids of equal length with the same transit time of blood through each sinusoid. The simulation studies were designed to mimic a single pass liver perfusion experiment with varying steady state input concentrations of drug at a constant blood flow rate. Intrinsic metabolism and/or biliary excretion of substrates are assumed to be governed by an apparent unienzyme system which is designated as a "metabolizing enzyme" to simplify the model description. The important assumptions of this model are the same as previously described (22). Although the maximum capacities of the transporter ($V_{max,1}$) and the metabolizing enzyme ($V_{max,3}$) are assumed constant (equations 1 and 2, respectively), their activities at any given point x along the sinusoidal blood flow path of L ($0 \leq x \leq L$), $V_{max,1,x}$ and $V_{max,3,x}$, respectively, may vary in accordance to the zonal distribution patterns used in these simulations.

$$V_{\max,1} = \int_0^L V_{\max,1,x}dx \quad (1)$$

$$V_{\max,3} = \int_0^L V_{\max,3,x}dx \quad (2)$$

At steady state, the rate of drug disappearance over an increment dx from x can be described as follows.

$$Q\frac{dC_{s,x}}{dx} = \frac{1}{L}(CL_{2,x}f_tC_{t,x} - CL_{1,x}f_bC_{s,x}) \quad (3)$$

Q is the hepatic blood flow rate. $C_{s,x}$ and $C_{t,x}$ are drug concentrations in the sinusoid and the hepatocyte compartments at x, respectively. $CL_{1,x}$ is the uptake clearance of drug from the sinusoidal compartment into the hepatocyte compartment by both a carrier-mediated system and passive diffusion (equation 4), and $CL_{2,x}$ is the diffusional efflux clearance from hepatocytes into the sinusoid at x (equation 5).

$$CL_{1,x} = \frac{V_{\max,1,x}}{K_{m,1} + f_bC_{s,x}} + CL_{d,x} \quad (4)$$

$$CL_{2,x} = CL_{d,x} \quad (5)$$

$CL_{d,x}$ is the diffusional clearance at x. At steady state, the uptake rate of drug from sinusoidal blood into hepatocytes is equal to the sum of the efflux and intrinsic elimination rates from hepatocytes (equation 6).

$$CL_{1,x}f_bC_{s,x} = CL_{2,x}f_tC_{t,x} + CL_{3,x}f_tC_{t,x} \quad (6)$$

$CL_{3,x}$ is the intrinsic clearance at x as in equation 7.

$$CL_{3,x} = \frac{V_{\max,3,x}}{K_{m,3} + f_tC_{t,x}} \quad (7)$$

METHODS

Three different distribution patterns of the transporter and the metabolizing enzyme activities from the input (periportal) to the output (perivenous) regions of blood in the liver are described in Figure 1: a linear decrease (model 1), an even distribution (model 2), and a linear increase (model 3). Possible combinations of these three distribution patterns of the transporter and the metabolizing enzyme (a total of 9 pairs) were used for simulations.

Table 1. Reference Parameters for a Hypothetical Substrate

Q ml/min	$V_{max,1}$ mg/min	$K_{m,1}$ mg/ml	CL_d ml/min	$V_{max,3}$ mg/min	$K_{m,3}$ mg/ml	f_b	f_t
10	10	1	0.01	10	10	1	1

The reference conditions (Table 1) and changes in parameter values were designed such that uptake process of drug plays an important role in determining clearance (CL) over a range of steady-state input concentrations ($C_{s,0}$), and heterogeneous distribution patterns of the transporter and metabolizing enzyme activities can produce significant effects on drug disposition in blood and hepatocytes. Q and CL_d were kept constant at 10 ml/min and 0.01 ml/min, respectively.

The rate of drug disappearance in the sinusoid compartment over an increment dx from x was numerically calculated, using Euler's method (23) with 500 iterative incremental steps (dx = 1/500 of flow path). The hepatic clearance was estimated using equation 8.

$$CL = Q\frac{C_{s,0} - C_{s,L}}{C_{s,0}} \quad (8)$$

The concentration gradient profiles of the drug in the sinusoidal blood and hepatocyte compartments were simulated, at a constant $C_{s,0}$ of 1 mg/ml. $C_{s,0}$ of 1 mg/ml was chosen, since at this concentration there were significant differences in CL and concentration gradient profiles as a result of distributional heterogeneities in the transporter and the metabolizing enzyme activities without significant saturation of the transporter activity.

RESULTS

Effects of Changes in $K_{m,1}$ and $V_{max,1}$

Figure 2 demonstrates the changes in CL as a function of $C_{s,0}$ with a declining $V_{max,1,x}$ and various distribution patterns

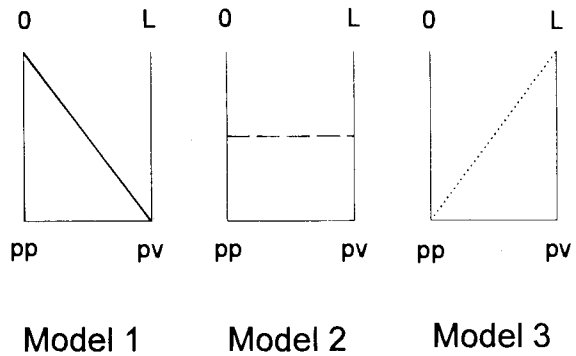

Fig. 1. Distribution patterns of the transporter and the metabolizing enzyme activities along the sinusoidal flow path. In each model, $V_{max,1}$ and $V_{max,3}$ are held constant, while the activities (y-axis) at different x (x-axis) are varied along the sinusoidal blood flow path from input (0) to output (L) in the liver; pp and pv represent the periportal and perivenous regions, respectively.

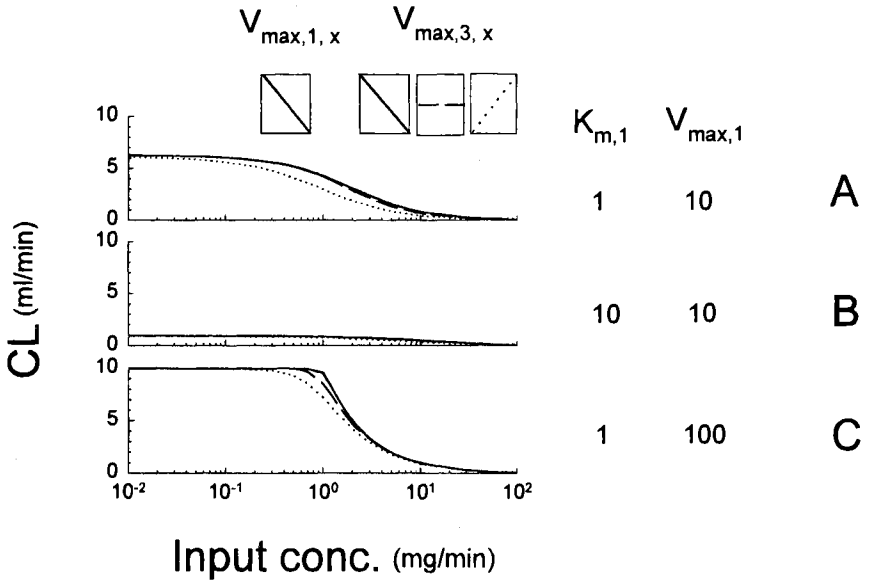

Fig. 2. Relationship between $C_{s,0}$ and CL with a linearly declining $V_{max,1,x}$ and various distribution patterns of $V_{max,3,x}$ at the reference conditions (Table 1, A), at 10 fold higher $K_{m,1}$ or $V_{max,1}$ (B, C). In this and subsequent figures, the units for K_m and V_{max} are mg/ml and mg/min, respectively.

of $V_{max,3,x}$, at different $K_{m,1}$ and $V_{max,1}$. Significant changes in CL were observed at different $K_{m,1}$ or $V_{max,1}$ (Fig. 2, B and C), compared with that under the reference conditions (Fig. 2, A), irrespective of zonal heterogeneities. A declining $V_{max,3,x}$ produced the highest CL, while an ascending $V_{max,3,x}$ estimated the lowest. The simulations of blood and hepatocyte concentration gradient profiles at $C_{s,0}$ of 1 mg/ml along the length normalized sinusoidal flow path are shown in Figure 3. The concentration of drug in the sinusoid gradually declined along the acinar pathway, with pronounced differences due to the distribution patterns of $V_{max,3,x}$ when $V_{max,1,x}$ and CL_1 were much larger than $V_{max,3,x}$ and CL_3. Significant accumulation of drug in hepatocyte compared with in neighboring blood was observed. There were also distinct differences in the tissue concentration gradient profiles due to the distribution patterns of $V_{max,3,x}$. An

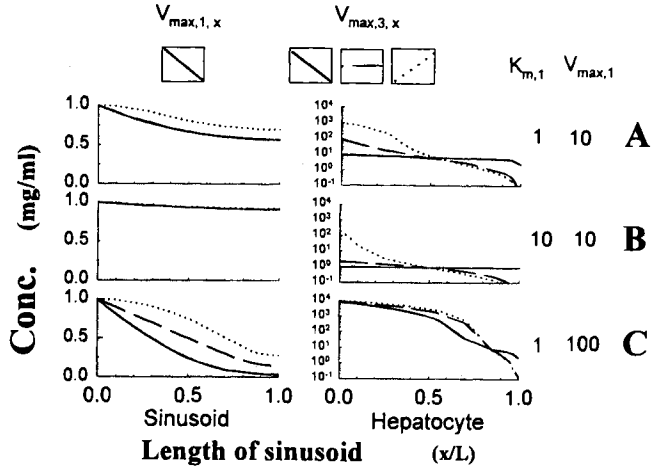

Fig. 3. Sinusoidal blood and hepatocyte tissue concentration gradient profiles along the length-normalized flow path for the conditions described in the Figure 2 legend at $C_{s,0}$ = 1 mg/ml.

opposite distribution pattern of $V_{max,1,x}$ to $V_{max,3,x}$ produced the sharpest decline of tissue concentrations from the periportal region across the acinus, while there was only a slight decrease in tissue concentrations with the same distribution patterns of $V_{max,1,x}$ and $V_{max,3,x}$ (Fig. 3, A and B) except at higher $V_{max,1}$ (Fig. 3, C). The evenly distributed $V_{max,3,x}$ produced a tissue drug concentration profile somewhere between the other two conditions. These effects became less evident with an increasing $V_{max,1}$, where a significant drug accumulation in the periportal region followed by a sharp decrease was seen with all three distribution patterns of $V_{max,3,x}$.

The differences in CL caused by the zonal heterogeneities of $V_{max,3,x}$ were less evident with an evenly distributed $V_{max,1,x}$ (data not presented) than with a declining $V_{max,1,x}$. Even if the blood concentration gradient profiles had distinct shapes, depending on distribution patterns of $V_{max,3,x}$, the drug concentrations at the blood outlet were not different from one another. In these simulations, in some cases, hepatocyte drug concentrations increased along the flow path.

An ascending $V_{max,1,x}$ with a declining $V_{max,3,x}$ produced the lowest CL estimates among the three different distribution patterns of the metabolizing enzyme, although the differences were small (Fig. 4). The blood concentration profiles did not vary much except at higher $V_{max,1,x}$ (Fig. 5). The tissue drug concentration increased most dramatically within a short distance from the periportal region at ascending $V_{max,1,x}$ and $V_{max,3,x}$. The highest tissue accumulation at the perivenous region was observed with a descending $V_{max,3,x}$, regardless of the magnitude of CL_1.

Effects of Changes in $K_{m,3}$ and $V_{max,3}$

There were no significant changes in CL by altering $K_{m,3}$ or $V_{max,3}$, although the various distribution patterns of $V_{max,3,x}$ caused significant differences in CL, except at higher $V_{max,3}$, or at evenly distributed $V_{max,1,x}$. In general, altering $V_{max,3}$, distribu-

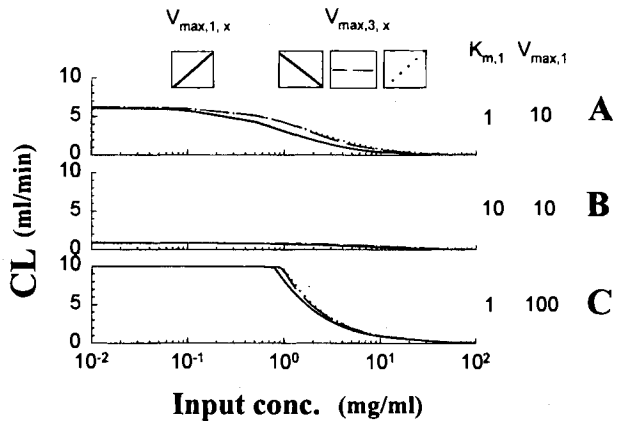

Fig. 4. Relationship between $C_{s,0}$ and CL with a linearly increasing $V_{max,1,x}$ and various distribution patterns of $V_{max,3,x}$ at the reference values (A), at 10 fold higher $K_{m,1}$ or $V_{max,1,x}$ (B, C).

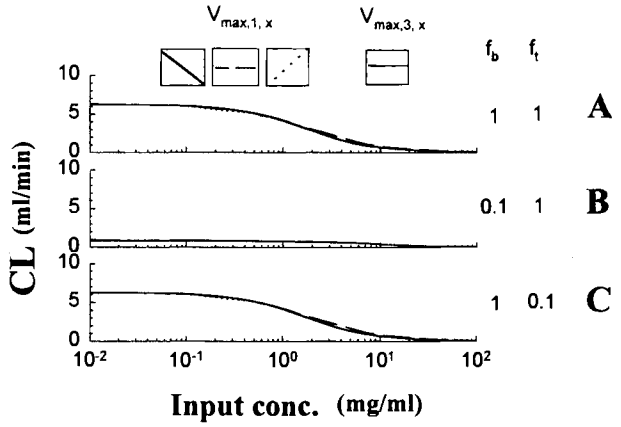

Fig. 6. Relationship between $C_{s,0}$ and CL with various distribution patterns of $V_{max,1,x}$ and an evenly distributed $V_{max,3,x}$ at the reference conditions (A), at 10 fold lower f_b or f_t (B, C).

tion patterns produced similar effects on concentration gradient profiles in tissue as those produced by altering the distribution patterns of $V_{max,1,x}$, although blood concentration profiles were different (data not presented).

Effects of Changes in f_b and f_t

Figure 6 illustrates the effects of f_b and f_t on CL, with various $V_{max,1,x}$ distribution patterns and an evenly distributed $V_{max,3,x}$. At lower f_b, a marked decrease in CL was seen (Fig. 6, B), whereas a decrease of f_t did not affect CL (Fig. 6, C). A decrease of f_b diminished the effects of the distribution patterns of $V_{max,1,x}$ on blood and tissue concentration gradient profiles (Fig. 7, B). A decrease of f_t did not affect blood concentrations but increased tissue concentrations (Fig. 7, C). It is interesting to note that a 10 fold decrease in f_b reduced the tissue concentration more than 10 fold, compared with that under reference conditions (Fig. 7, A), while changes in f_t produced the same magnitude of change in tissue concentrations. This reflects the linear relationship between $C_{t,x}$ and f_t and the exponential relationship between $C_{s,x}$ and f_b (see Appendix in accompanying paper).

Comparison of CL Among Different Distribution Patterns of $V_{max,1,x}$ and $V_{max,3,x}$

Figure 8 illustrates the relationships between $C_{s,0}$ and CL ratios obtained by normalizing CL estimates with the different distribution patterns of $V_{max,1,x}$ and $V_{max,3,x}$, by those obtained with an evenly distributed $V_{max,3,x}$, under the reference conditions. The same distribution patterns of $V_{max,1,x}$ and $V_{max,3,x}$ produced the highest CL and the opposite ones showed the lowest. With an evenly distributed $V_{max,1,x}$, both declining and ascending $V_{max,3,x}$ produced lower CL estimates than that with an evenly distributed $V_{max,3,x}$. Relative CL differences among various distribution patterns became more significant as $C_{s,0}$ increased.

DISCUSSION

The present simulations demonstrated that the spatial distribution heterogeneities of the sinusoidal membrane transporter

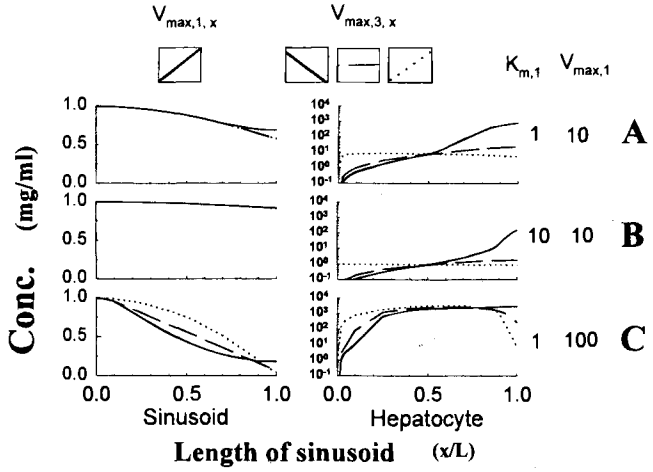

Fig. 5. Sinusoidal blood and hepatocyte tissue concentration gradient profiles along the length-normalized flow path for the conditions described in the Figure 4 legend at $C_{s,0}$ = 1 mg/ml.

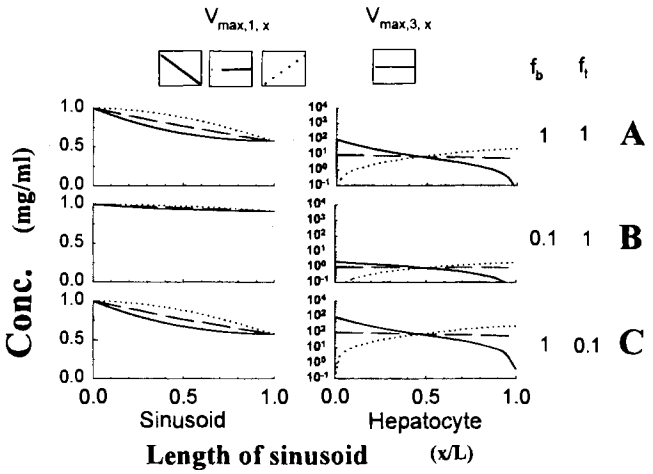

Fig. 7. Sinusoidal blood and hepatocyte tissue concentration gradient profiles along the length-normalized flow path for the conditions described in the Figure 6 legend at $C_{s,0}$ = 1 mg/ml.

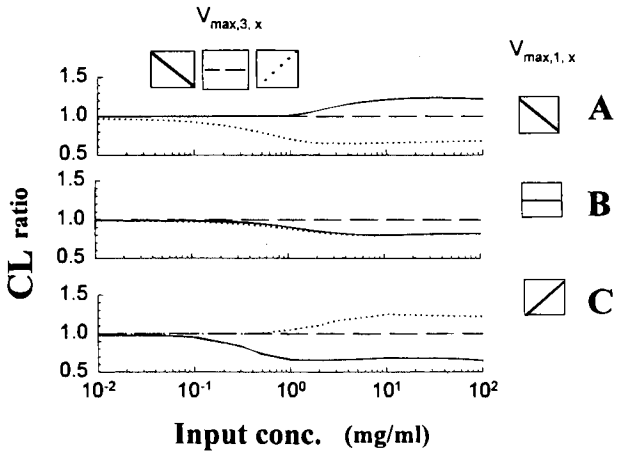

Fig. 8. Relationship between $C_{s,0}$ and *CL* ratio: *CL* with different distribution patterns of $V_{max,1,x}$ and $V_{max,3,x}$ was normalized by the *CL* obtained with an evenly distributed $V_{max,3}$, using the reference parameter values.

and the metabolizing enzyme (or hepatobiliary transporter) could significantly affect *CL*, as well as substrate concentration gradient profiles in the sinusoidal blood and hepatocytes. These effects were dependent on the capacities and affinities of the transporter and the metabolizing enzyme. These findings are most relevant for our understanding of the hepatic disposition and clearance of polar compounds, such as ionized organic anions and cations, many of which undergo hepatic uptake and hepatobiliary elimination by facilitated transport processes (18,24).

Previous studies have demonstrated that in the absence of a transport barrier, the distribution patterns of the metabolizing enzyme along the sinusoidal flow path do not affect the overall organ elimination of a substrate (25) under linear conditions. However, in the presence of a diffusional barrier between blood and hepatocytes, Sato *et al.* (15) found, also under linear conditions, that the more skewed distribution of the metabolizing enzyme produced the lower extraction ratio of drug. The present simulation studies further investigated the effects of zonal heterogeneities in transporter as well as metabolizing enzyme on *CL*, assuming nonlinear conditions. An evenly distributed transporter activity with decreasing or increasing metabolizing enzyme distribution patterns along the sinusoidal flow path produced a lower *CL* than that observed with an evenly distributed metabolizing enzyme activity (Fig. 8B). This is similar to the findings of Sato *et al.* (15). However, when zonal heterogeneities occurred in both transporter and metabolizing enzyme activities, the same distribution patterns of transporter and metabolizing enzyme activities produced the highest *CL* estimates, while the opposite patterns produced the lowest estimates (Fig. 8A, C). Interestingly, the effects of zonal heterogeneities in both processes on *CL* were not significant at the low input concentrations, regardless of distribution patterns, indicating that the magnitude of the effects of zonal heterogeneities of transporter and/or metabolizing enzyme on *CL* can be concentration-dependent as well.

Simulation studies on the effects of diffusional clearance on blood and tissue concentration profiles of drug under linear conditions assuming no protein binding to blood and tissue components (26,27), suggested that with an evenly distributed metabolizing enzyme activity, tissue concentrations will always be lower than or at best close to blood concentrations at any point along the sinusoidal flow path. However, multiple indicator dilution studies on the hepatic transport of rubidium (28) indicated that the drug accumulated in hepatocytes against its concentration gradient, when the uptake rate constant of the substrate was greater than the efflux rate constant. The present simulations demonstrated that the tissue concentrations of drugs could be much higher than those in the neighboring sinusoidal blood as a result of a facilitated transport system. Interestingly, tissue concentration gradient profiles under the present conditions were very similar to the transporter distribution patterns (Figures 3 and 5), except in the case of an evenly distributed transporter; in the case of evenly distributed transport activities, the metabolizing enzyme distribution affected the localization of drug within hepatocytes.

The changes in tissue binding significantly affected the extent of drug accumulation in hepatocyte without altering clearance or concentration gradient profiles in the sinusoid, which agrees with previous simulations (26). Gumucio *et al.* (29) have examined the effects of blood albumin on the concentration of sulfobromophthalein (BSP) within hepatocytes of each acinar zone after a steady state infusion of BSP in rats. They found that BSP, perfused in the absence of albumin, generated distinct profiles of decreasing cellular concentrations from the periportal to the perivenous region; however, the addition of albumin in the perfusate significantly reduced the extraction ratio and distributed BSP more homogeneously throughout the acinus. The studies on the effects of blood protein binding (Figures 6 and 7) demonstrated that the extent of drug bound to blood components can affect not only the clearance, but also the zonal concentration gradient profiles of drug within hepatocytes. Since the present model assumes a constant f_b and f_t throughout the liver, further development of the model is needed to address the effects of nonlinear protein binding (30) in blood and/or tissue, in the presence of zonal heterogeneity of the capacity-limited transporter and metabolizing enzyme.

In conclusion, this simulation study has demonstrated that 1) zonal differences in the transporter and/or the metabolizing enzyme distribution patterns have significant effects on *CL*, and on blood and tissue concentration profiles, 2) the significance of the effects of zonal heterogeneities in the transporter and the metabolizing enzyme activities is dependent on the Michaelis-Menten parameters for those nonlinear processes, and 3) the extent of protein binding of drugs to blood or tissue components can significantly affect *CL* and/or the zonal concentration gradient profiles of drugs in the sinusoidal blood and/or hepatocytes.

REFERENCES

1. J. J. Gumucio. *Hepatology* **9**(1):154–160 (1989).
2. N. Katz and K. Jungermann. In "Hepatic transport and bile secretion: physiology and pathology" (N. Tavoloni and P. D. Berk, eds), Raven Press Ltd., New York, pp. 55–70 (1993).
3. K. Jungermann and N. Katz. *Physiol. Rev.* **69**:708–764(1989).
4. B. Quistorff. *Essays Biochem.* **25**:83–136 (1990).
5. J. J. Gumucio and E. E. Guibert. In "Hepatic transport and bile secretion: physiology and pathology" (N. Tavoloni and P. D. Berk, eds), Raven Press Ltd., New York, pp. 71–82 (1993).
6. G. M. M. Groothuis and D. K. F. Meijer. *Enzyme* **46**:94–138 (1992).
7. H. J. Burger, R. Gebhardt, C. Mayer, and D. Mecke. *Hepatology.* **9**(1):22–28 (1989).

8. G. M. M. Groothuis, K. P. T. Keulemans, M. J. Hardonk, and D. K. F. Meijer. *Biochem. Pharmacol.* **32**(20):3069–3078 (1983).
9. G. M. M. Groothuis, J. G. Weitering, K. P. T. Keulemans, M. J. Hardonk, D. Mulder, and D. K. F. Meijer. *Naunyn-Schmiedeberg's Arch. Pharmacol.* **322**:310–318 (1983).
10. H. Saiki, E. T. Chan, E. Wong, W. Yamamuro, M. Ookhtens, and N. Kaplowitz. *J. Biol. Chem.* **267**:192–196 (1992).
11. I. Braakman, G. M. M. Groothuis, and D. K. F. Meijer. *Hepatology.* **7**(5):849–855 (1987).
12. J. J. Gumucio, D. L. Miller, M. D. Krauss, and C. C. Zanolli. *Gastroenterology.* **80**:639–646 (1981).
13. P. V. D. Sluijs, I. Braakman, D. K. F. Meijer, and G. M. M. Groothuis. *Hepatology.* **8**(6):1521–1529 (1988).
14. C. A. Goresky, G. G. Bach, and C. P. Rose. *Am. J. Physiol.* **244**:G215–G232 (1983).
15. H. Sato, Y. Sugiyama, S. Miyauchi, Y. Sawada, T. Iga, and M. Hanano. *J. Pharm. Sci.* **75**(1):3–8 (1986).
16. M. E. Morris and K. S. Pang. *J. Pharmacokin. Biopharm.* **15**(5):473–496 (1987).
17. M. E. Morris, V. Yuen, and K. S. Pang. *J. Pharmacokin. Biopharm.* **16**(6):633–656 (1988).
18. D. K. F. Meijer, W. E. M. Mol, M. Muller, and G. Kurz. *J. Pharmacokin. Biopharm.* **18**:35–70 (1990).
19. R. H. Moseley, S. M. Jarose, and P. Permoad. *Am. J. Physiol.* **263**:G775–G785 (1992).
20. S. Keiding, S. Johansen, K. Winkler, K. Tønnesen, and N. Tygstrup. *Am. J. Physiol.* **230**(5):1302–1313 (1976).
21. J. Reichen and G. Paumgartner. *Gastroenterology.* **68**:132–136 (1975).
22. Y. Kwon and M. E. Morris. *Pharm. Res.* (companion article).
23. R. B. Hornbeck. In Numerical Methods, Quantum Publishers, Inc., New York, 1975, pp. 185–226.
24. M. Yamazaki, H. Suzuki, and Y. Sugiyami. *Pharm. Res.* **13**:497–513 (1996).
25. K. S. Pang and R. N. Stillwell. *J. Pharmacokin. Biopharm.* **11**:451–468 (1983).
26. I. A. M. de Lannoy and K. S. Pang. *Drug. Metab. Dispos.* **14**:513–520 (1986).
27. I. A. M. DeLannoy and K. S. Pang. *Drug Metab. Dispos.* **15**(1):51–58 (1987).
28. C. A. Goresky, G. G. Bach, and B. E. Nadeau. *J. Clin. Invest.* **52**:975–990 (1973).
29. P. L. Gumucio, J. J. Gumucio, J. A. P. Wilson, C. Cutter, M. Krauss, R. Caldwell, and E. Chen. *Am. J. Physiol.* **246**:G86–G95 (1984).
30. X. Xu, P. Selick, and K. S. Pang. *J. Pharmacokin. Biopharm.* **21**:43–74 (1993).